

# A new method to study the EMC Effect using the $F_2^n$ structure function

H. Szumila-Vance<sup>1</sup>, I. Cloet<sup>2</sup>, C. Keppel<sup>1</sup>, S. Escalante<sup>3</sup>, N. Kalantarians<sup>3</sup>

<sup>1</sup>Thomas Jefferson National Accelerator Facility, Newport News, VA

<sup>2</sup>Argonne National Laboratory, Argonne, IL

<sup>3</sup>Virginia Union University, Richmond, VA

## Abstract

The persistently mysterious deviations from unity of the ratio of nuclear target structure functions to those of deuterium as measured in deep inelastic scattering (termed the EMC effect) have become the canonical observable for studies of nuclear medium modifications to free nucleon structure in the valence regime. The structure function of the free proton is well known from numerous experiments spanning decades. The free neutron structure function, however, has remained difficult to access. It has recently been extracted in a systematic study of the global data within a parton distribution function extraction framework, and is available from the CTEQ-Jefferson Lab (CJ) Collaboration. Here we leverage the latter to introduce a new method to study the EMC Effect in nuclei by re-examining existing data, now determining the magnitude of the medium modifications to the free neutron and proton structure functions independently. From the extraction of the free neutron from world data, it is possible to examine the nuclear effects in deuterium and their contribution to our interpretation of the EMC Effect.

## 1 Introduction

We chose to use the SLAC E139 data set because it is the most complete published list of cross sections available. From the initial cross sections given, we converted the absolute cross section to the structure function by using the kinematics and R1990 fitting.

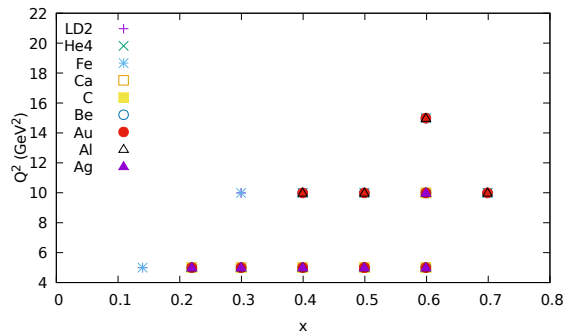
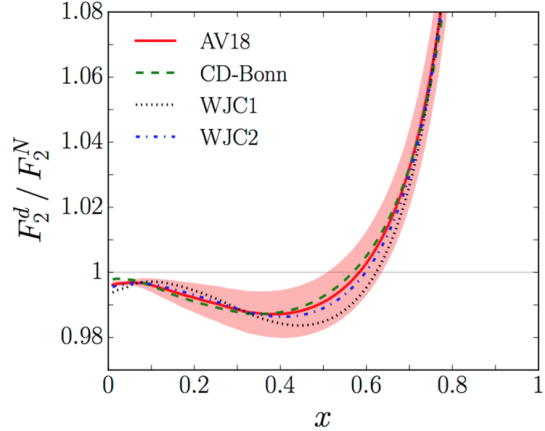


Figure 1

## 2 Theory predictions using nuclear matter

Discussion points: predicted d/n and d/p ratios, interpretations in quark distributions, emc effects in deuterium



**Figure 2**

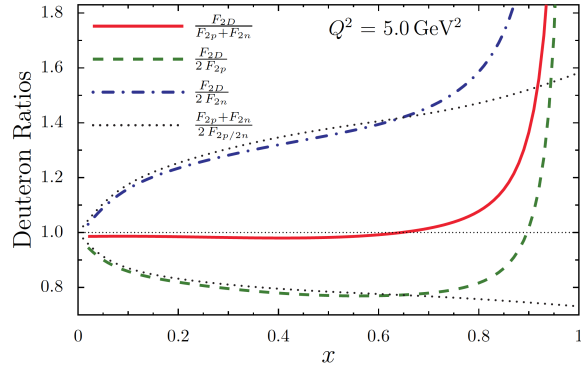


**Figure 3**

## 3 $F_2^n$ extraction and the CJ15 fit

We need to point to CJ and how the world data was extracted.

### 3.1. $Q^2$ dependence

## 4 Structure function extraction from the E139 cross sections

Discuss the input cross section, conversion to F2A and the iso-scalar correction.

$$F_2 = \frac{d^2\sigma}{d\Omega dE'} \frac{1+R}{1+\epsilon R} \frac{K\nu}{4\pi^2\alpha\Gamma(1+\nu^2/Q^2)} \quad (1)$$

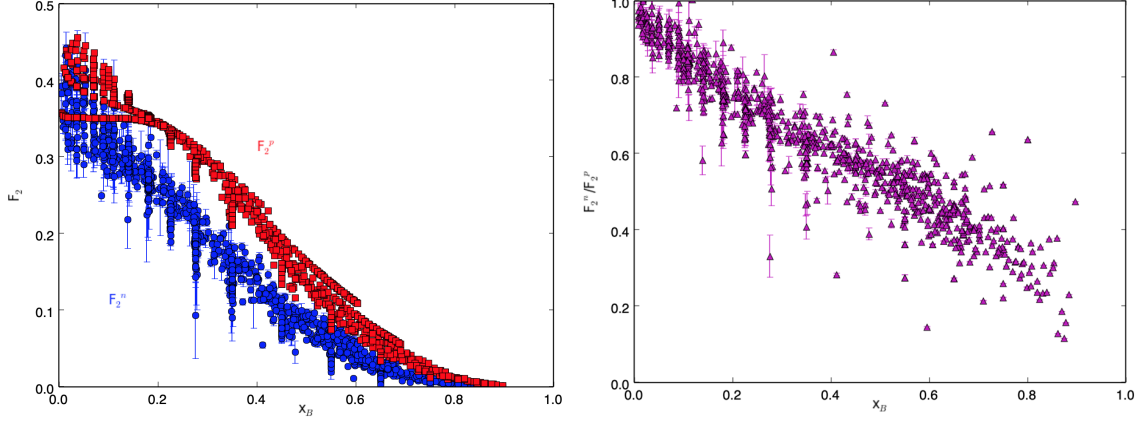


**Figure 4:** Left: The extracted  $F_2^n$  from the world DIS data is shown in blue, and the  $F_2^p$  from the NMC global fit is shown in red for the same corresponding  $x_B$  and  $Q^2$ . Right: The ratio of the  $F_2^n / F_2^p$  from the left is shown as a function of  $x_B$ .

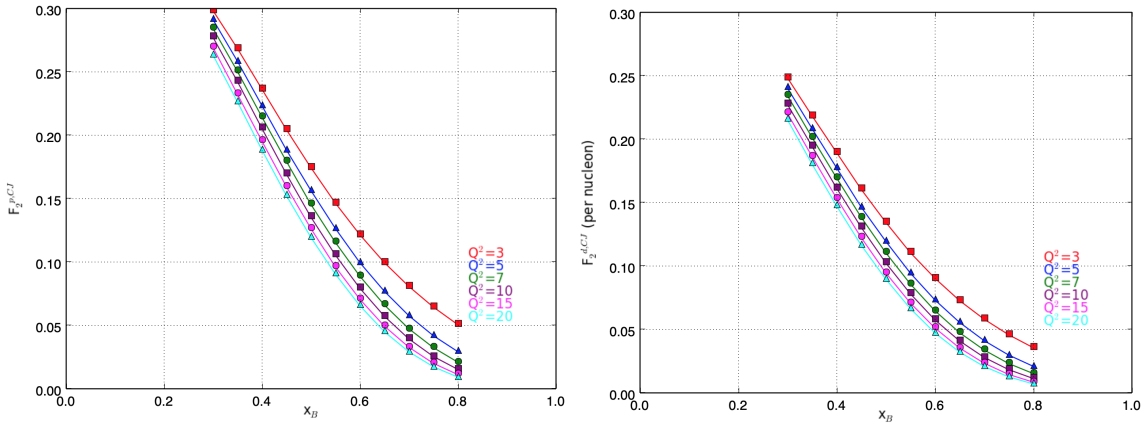


**Figure 5:** Left: The proton structure function from the CJ15 fit is shown as a function of  $x_B$  for various fixed  $Q^2$ . Right: The deuteron structure function from the CJ15 fit is shown as a function of  $x_B$  for various fixed  $Q^2$ .

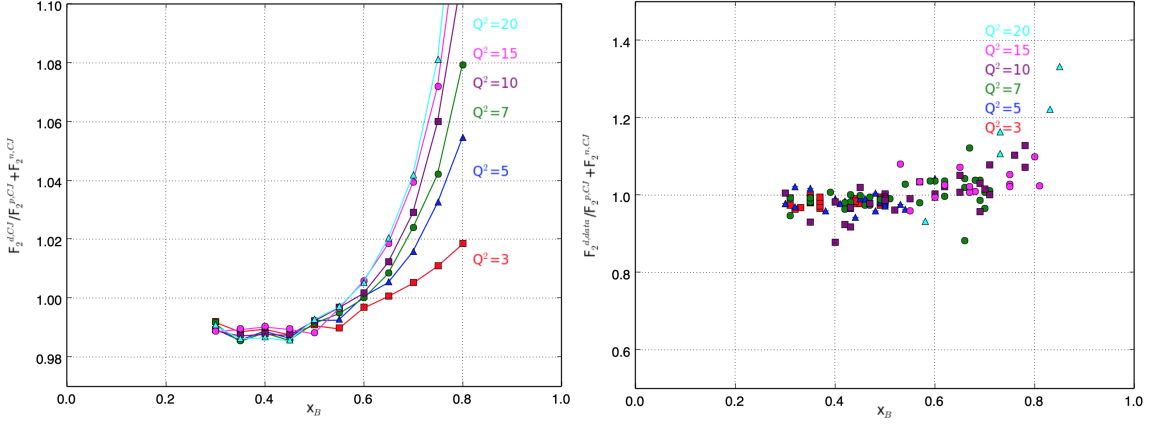


**Figure 6:** Left: The deuteron structure function divided by the sum of the free proton and free neutron structure functions from the CJ15 fit is shown for various  $Q^2$ . This ratio roughly shows the magnitude of the nuclear effects in the deuteron. The  $Q^2$  dependence shows significant spread above  $x_B = 0.6$  where the ratio begins to increase. Right: The global Whitlow deuterium data from SLAC [7] is shown divided by the sum of the free proton and free neutron structure functions from the CJ15 fit.

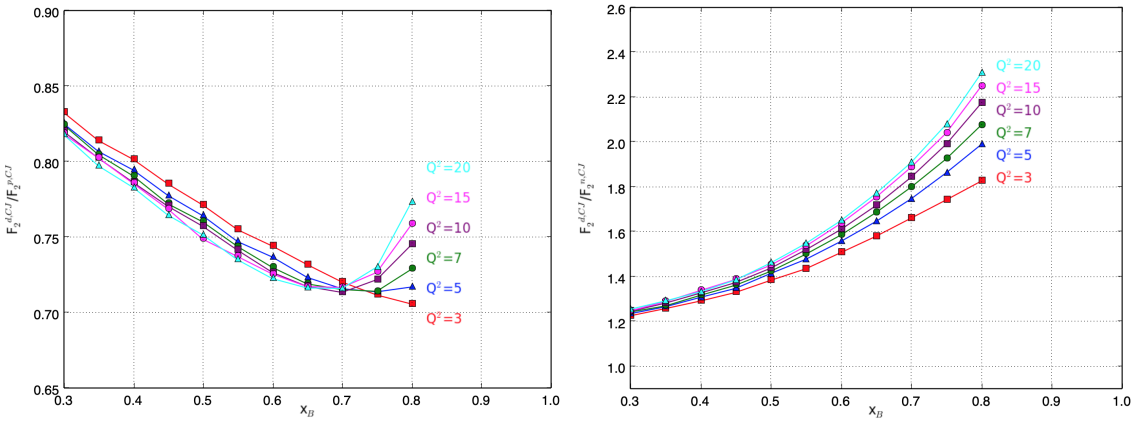


**Figure 7:** Left: The deuterium structure function from the CJ15 fit is shown as a ratio to the proton structure function from CJ15 for various  $Q^2$ . Right: The deuterium structure function from the CJ15 fit is shown as a ratio to the neutron structure function from CJ15 for various  $Q^2$ .

$$\epsilon = \left(1 + 2 \frac{v^2 + Q^2}{Q^2} \tan^2 \frac{\theta}{2}\right)^{-1} \quad (2)$$

$$K = \frac{W^2 - M^2}{2M} \quad (3)$$

$$\Gamma = \frac{\alpha K E'}{2\pi^2 Q^2 E (1 - \epsilon)} \quad (4)$$

$$f_{iso}^A = \frac{\frac{1}{2}(1 + F_2^n/F_2^p)}{\frac{1}{A}(Z + (A - Z)F_2^n/F_2^p)} \quad (5)$$

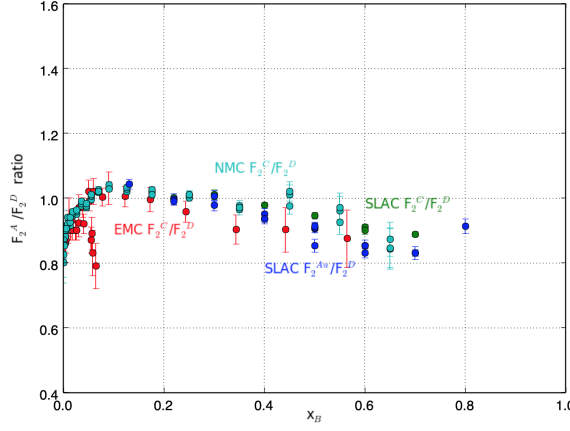


**Figure 8:** The published structure function ratios per nucleon for carbon and gold are shown from SLAC, NMC, and the EMC experiments.

## 5 General observations

## 6 Deuterium nuclear effects and heavier nuclei

### 6.1. Deuterium

plots: include d/n or n/d of Whitlow+BONUS to show Q2 dependency

### 6.2. Heavier nuclei

## 7 Conclusions

## 8 Acknowledgments

The authors would like to thank Shujie Li for constructing the most complete world  $F_2^n$  data set to date and Alberto Accardi and Wally Melnitchouk for providing crucial insights and interpretations for this analysis.

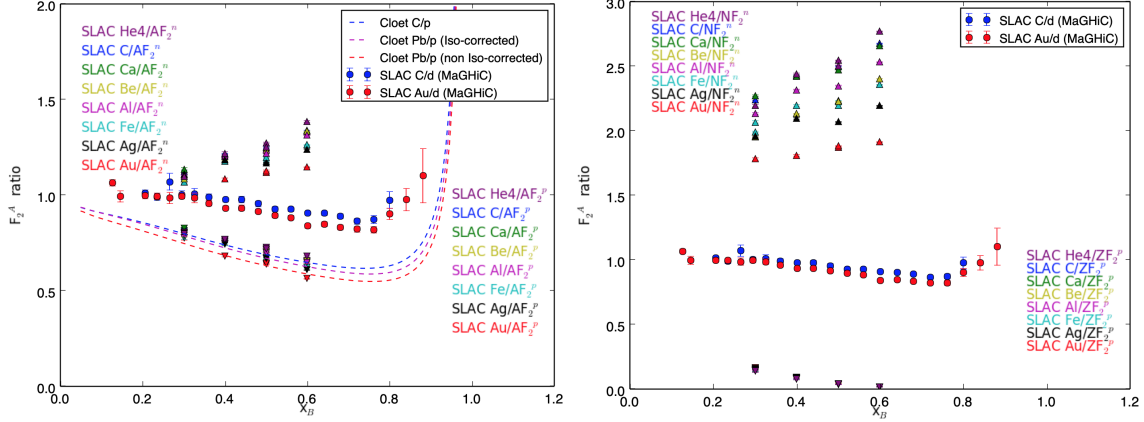


**Figure 9:** Left:  $F_2^A$  calculated from the published SLAC E139 cross sections is taken as a ratio per nucleon to  $F_2^n$  and  $F_2^p$ , separately. The published EMC ratios for carbon and gold [9] are shown for reference as  $F_2^A / F_2^n$  per nucleon. Theory predictions for the  $F_2^A$  structure function per nucleon as a ratio to  $F_2^p$  are shown. Right:  $F_2^A$  calculated from the published SLAC E139 cross sections is taken as a ratio per neutron or proton and  $F_2^n$  and  $F_2^p$ , separately. The published EMC ratios for carbon and gold [9] are shown for reference.

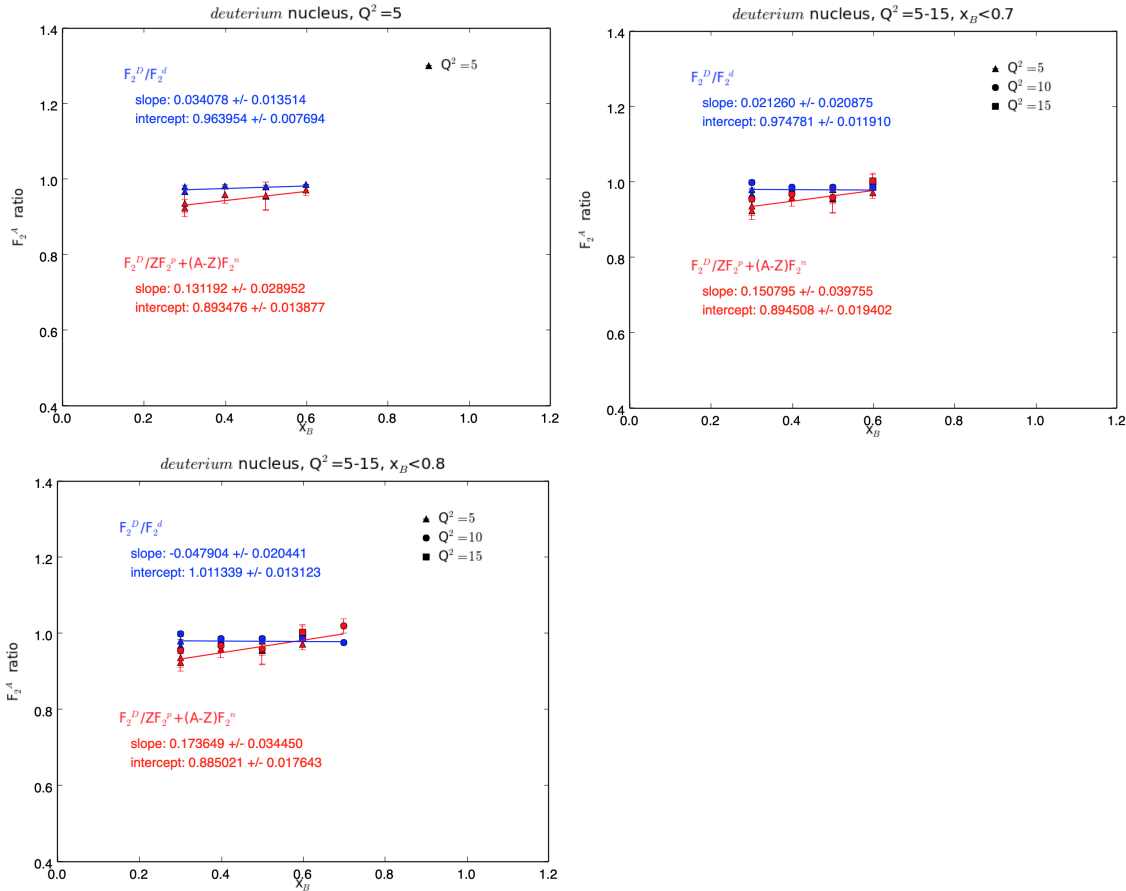


**Figure 10:** Linear fits to the deuterium target data with cuts on  $Q^2$  and  $x_B$ .

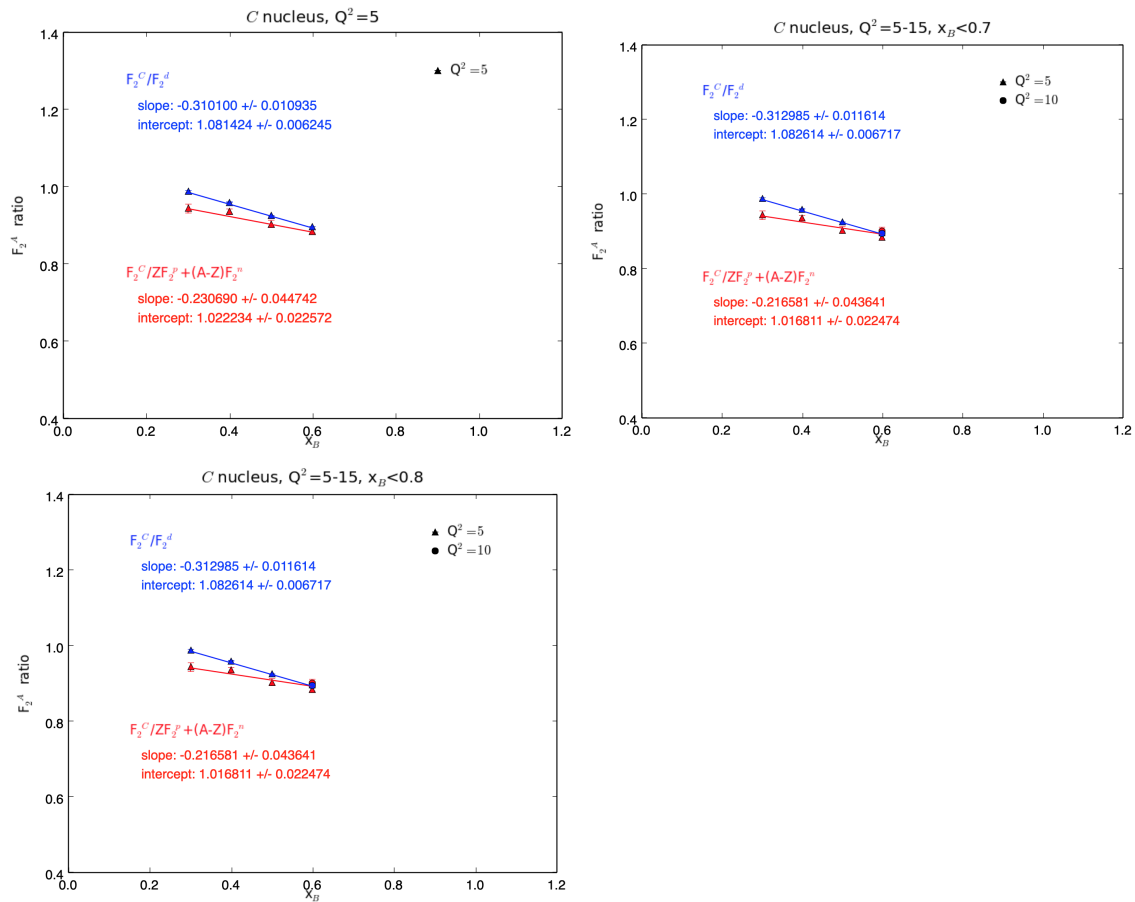


**Figure 11:** Linear fits to the  $C$  target data with cuts on  $Q^2$  and  $x_B$ .

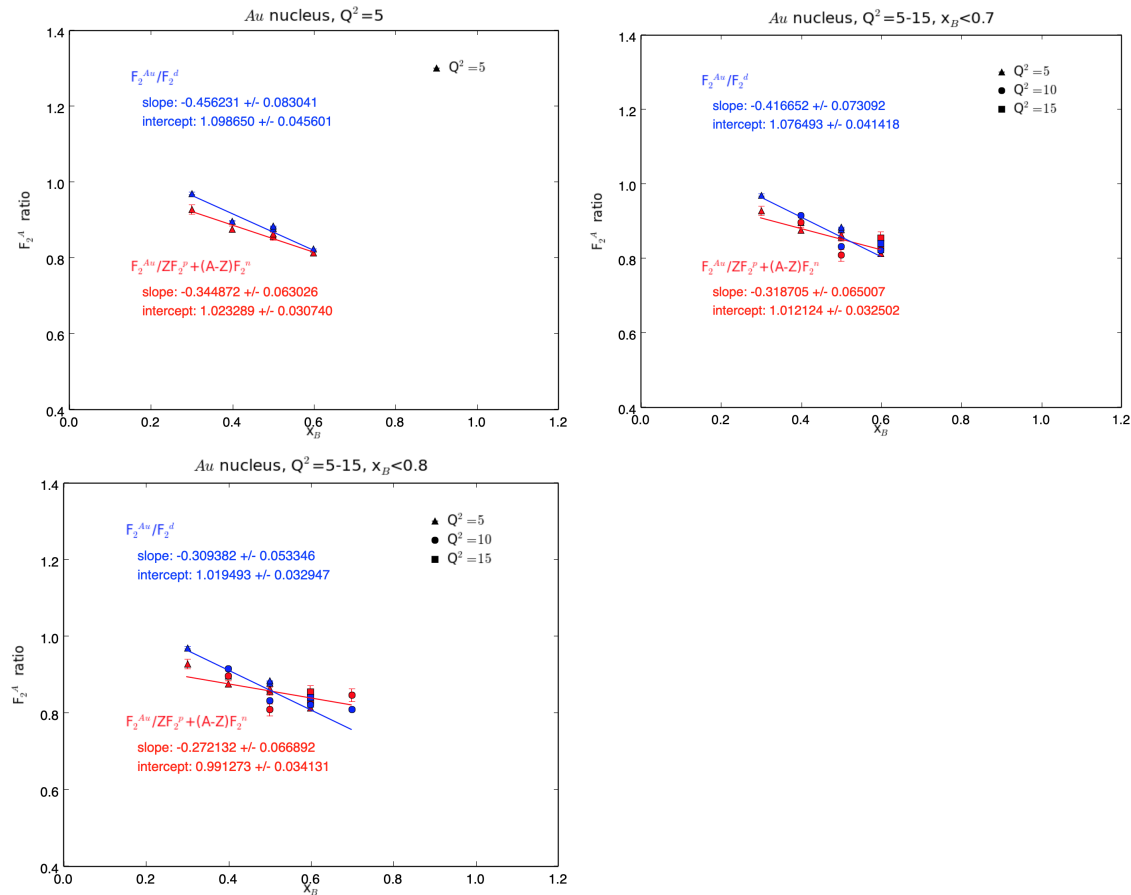


**Figure 12:** Linear fits to the  $Au$  target data with cuts on  $Q^2$  and  $x_B$ .

**Table 1:** Summary of linear fits to  $x_B$  where  $Q^2 = 5$ .

Nucleus	A/d slope	A/d intercept	A/(n+p) slope	A/(n+p) intercept
deuterium	0.034078+/- 0.013514	0.963954+/- 0.007694	0.131192+/- 0.028952	0.893476+/- 0.013877
He4	-0.139559+/- 0.041514	1.010444+/- 0.023729	-0.054561+/- 0.053741	0.947196+/- 0.027083
Be	-0.153575+/- 0.004225	1.020754+/- 0.002375	-0.064459+/- 0.041653	0.955925+/- 0.020121
C	-0.310100+/- 0.010935	1.081424+/- 0.006245	-0.230690+/- 0.044742	1.022234+/- 0.022572
Al	-0.308688+/- 0.058075	1.074479+/- 0.032618	-0.241920+/- 0.085474	1.021834+/- 0.042052
Ca	-0.327402+/- 0.048885	1.085172+/- 0.027035	-0.27227+/- 0.051774	1.037505+/- 0.025103
Fe	-0.368335+/- 0.041561	1.085849+/- 0.022646	-0.286425+/- 0.062250	1.024809+/- 0.029771
Ag	-0.423013+/- 0.087616	1.119710+/- 0.048607	-0.360732+/- 0.113255	1.068858+/- 0.055132
Au	-0.456231+/- 0.083041	1.098650+/- 0.045601	-0.344872+/- 0.063026	1.023289+/- 0.030740

**Table 2:** Summary of linear fits to  $x_B$  where  $Q^2 = 5 - 15$  and  $x_B < 0.7$ .

Nucleus	A/d slope	A/d intercept	A/(n+p) slope	A/(n+p) intercept
deuterium	0.021260+/- 0.020875	0.974781+/- 0.011910	0.150795+/- 0.039755	0.894508+/- 0.019402
He4	-0.118090+/- 0.035769	0.997067+/- 0.020596	-0.016222+/- 0.045129	0.931353+/- 0.023103
Be	-0.197454+/- 0.083778	1.035493+/- 0.048067	-0.059106+/- 0.030303	0.953386+/- 0.015144
C	-0.312985+/- 0.011614	1.082614+/- 0.006717	-0.216581+/- 0.043641	1.016811+/- 0.022474
Al	-0.298244+/- 0.057500	1.070859+/- 0.032829	-0.210889+/- 0.056564	1.010775+/- 0.028368
Ca	-0.334267+/- 0.034303	1.088128+/- 0.019560	-0.247045+/- 0.051788	1.027656+/- 0.025990
Fe	-0.379082+/- 0.040058	1.085956+/- 0.022621	-0.257315+/- 0.043599	1.010276+/- 0.021402
Ag	-0.432939+/- 0.060259	1.124006+/- 0.034442	-0.338549+/- 0.081071	1.060178+/- 0.040839
Au	-0.416652+/- 0.073092	1.076493+/- 0.041418	-0.318705+/- 0.065007	1.012124+/- 0.032502

## References

- [1] A. Accardi, L. T. Brady, W. Melnitchouk, J. F. Owens and N. Sato, Phys.Rev. D93 (2016) 114017

**Table 3:** Summary of linear fits to  $x_B$  where  $Q^2 = 5 - 15$  and  $x_B < 0.8$ .

Nucleus	A/d slope	A/d intercept	A/(n+p) slope	A/(n+p) intercept
deuterium	-0.047904+/-0.020441	1.011339+/-0.013123	0.173649+/-0.034450	0.885021+/-0.017643
He4	-0.066610+/-0.025529	0.969128+/-0.015975	0.024671+/-0.050676	0.913125+/-0.026599
Be	-0.105347+/-0.056027	0.986067+/-0.035211	-0.016830+/-0.042937	0.934997+/-0.022080
C	—	—	—	—
Al	-0.268256+/-0.036285	1.054884+/-0.022384	-0.178675+/-0.057032	0.996550+/-0.029163
Ca	—	—	—	—
Fe	-0.265522+/-0.041894	1.026296+/-0.025600	-0.219929+/-0.048613	0.994104+/-0.024310
Ag	—	—	—	—
Au	-0.309382+/-0.053346	1.019493+/-0.032947	-0.272132+/-0.066892	0.991273+/-0.034131

- [2] J. Gomez *et al.*, “Measurement of the A-dependence of deep inelastic electron scattering,” Phys. Rev. D **49**, 4348 (1994). doi:10.1103/PhysRevD.49.4348
- [3] K. A. Griffioen *et al.*, “Measurement of the EMC Effect in the Deuteron,” Phys. Rev. C **92**, no. 1, 015211 (2015) doi:10.1103/PhysRevC.92.015211 [arXiv:1506.00871 [hep-ph]].
- [4] J. G. Rubin, J. Arrington, “A New Extraction of Neutron Structure Functions from Existing Inclusive DIS Data,” doi: 10.1063/1.3631528 [arXiv:1101.3506v2 [nucl-ex]].
- [5] L.W.Whitlow, SLAC-Report-357, Ph.D. Thesis, Stanford University, March 1990.
- [6] <https://www.slac.stanford.edu/exp/e139/E139.RESULTS>
- [7] [http://www.slac.stanford.edu/exp/e140/SIGMA.D2\\_357](http://www.slac.stanford.edu/exp/e140/SIGMA.D2_357)
- [8] Alekhin, S. I. and Kulagin, S. A. and Petti, R., “Nuclear effects in the deuteron and constraints on the  $d/u$  ratio,” Phys. Rev. D **96**, no. 5, 0054005 (2017) doi:10.1103/PhysRevD.96.054005 [arXiv:1704.00204].
- [9] S. Malace, D. Gaskell, D. W. Higinbotham and I. Cloet, “The Challenge of the EMC Effect: existing data and future directions,” Int. J. Mod. Phys. E **23**, no. 08, 1430013 (2014) doi:10.1142/S0218301314300136 [arXiv:1405.1270 [nucl-ex]].

## 9 Appendix

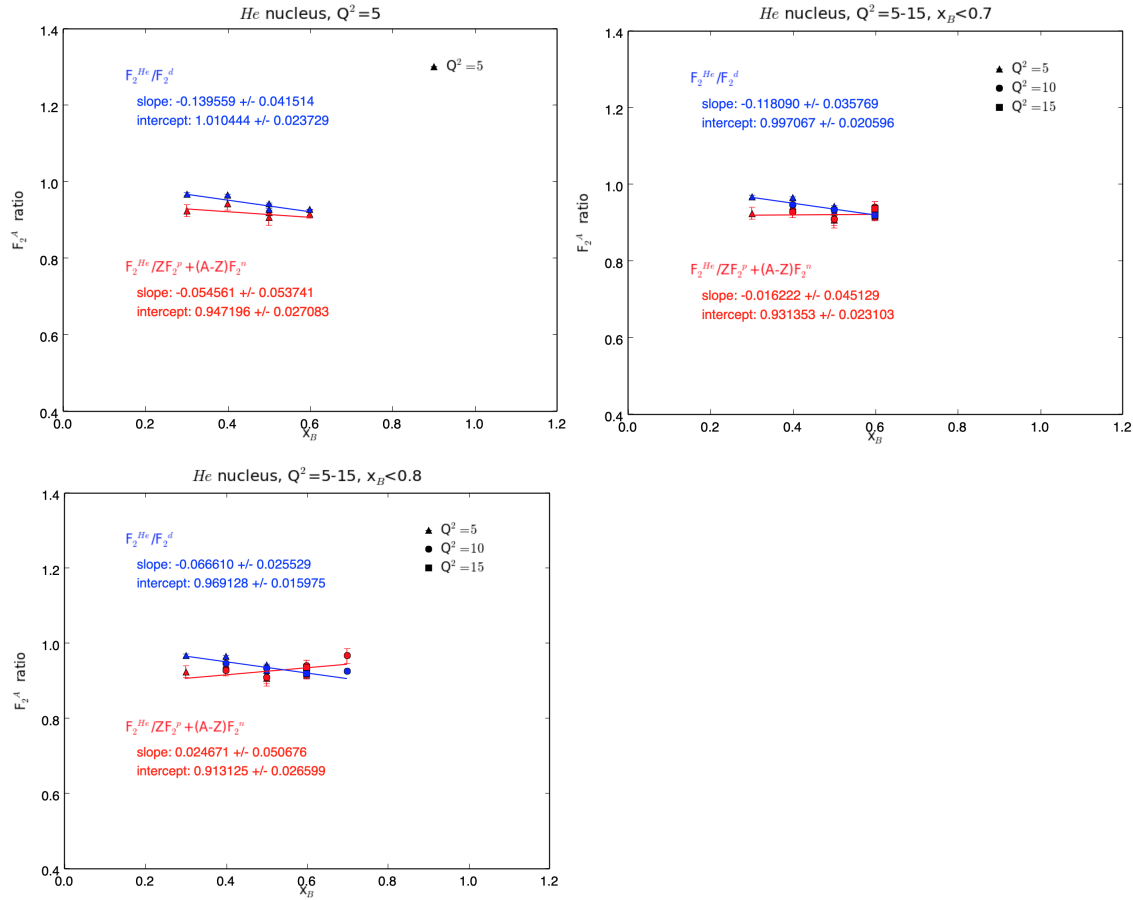


**Figure 13:** Linear fits to the He target data with cuts on  $Q^2$  and  $x_B$ .

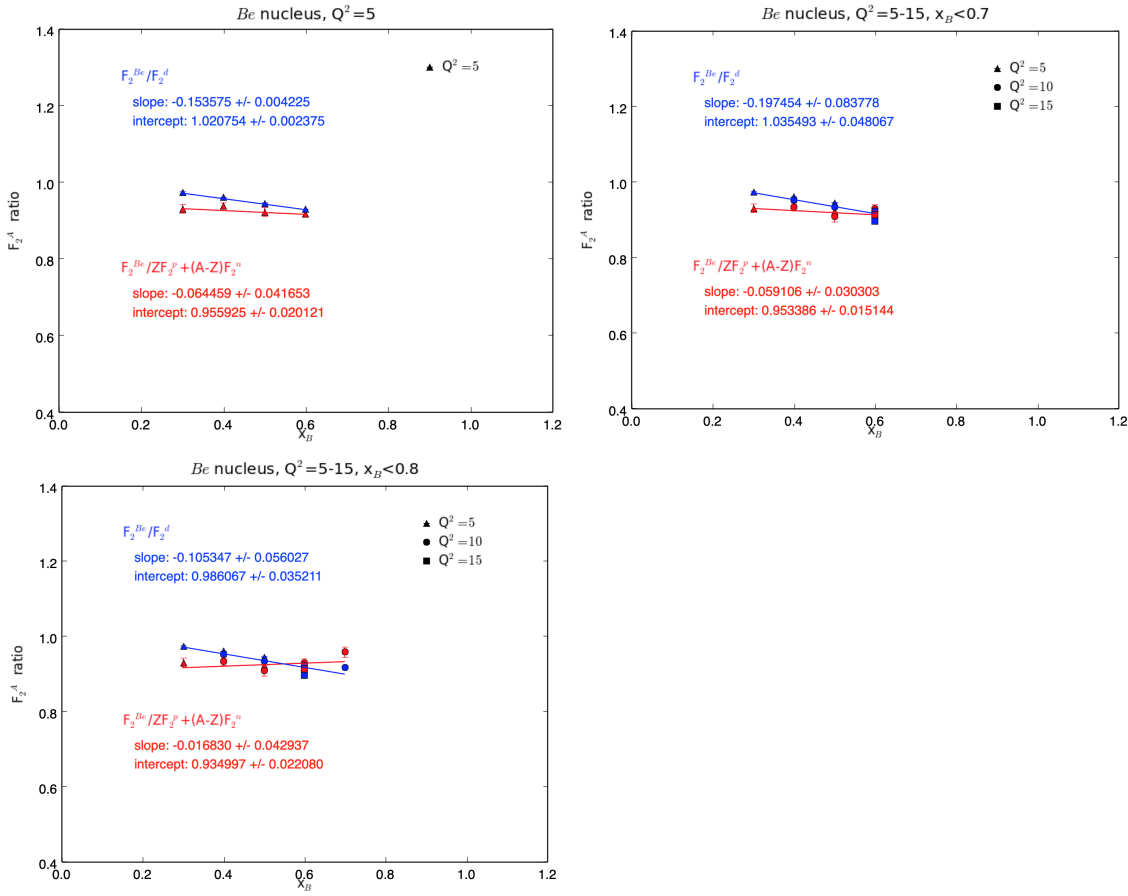


**Figure 14:** Linear fits to the Be target data with cuts on  $Q^2$  and  $x_B$ .

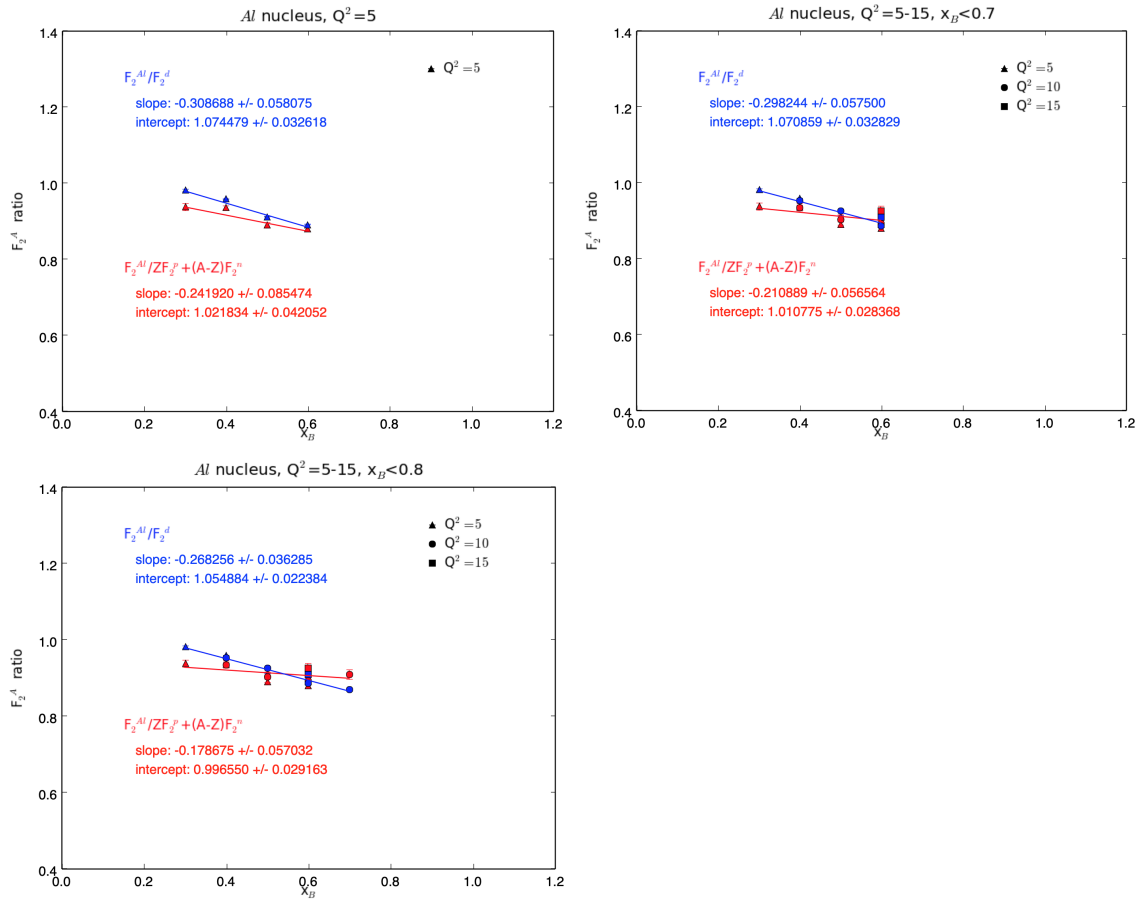


**Figure 15:** Linear fits to the Al target data with cuts on  $Q^2$  and  $x_B$ .

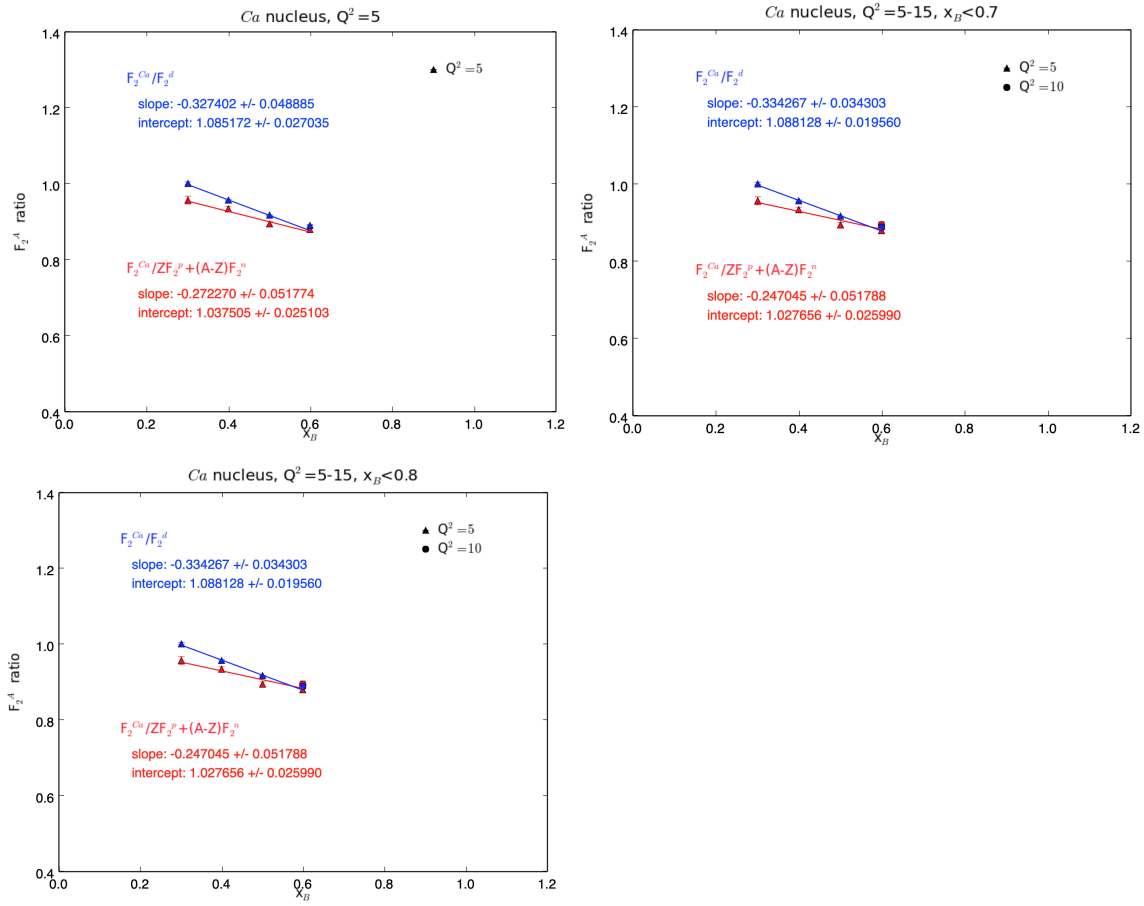


**Figure 16:** Linear fits to the Ca target data with cuts on  $Q^2$  and  $x_B$ .

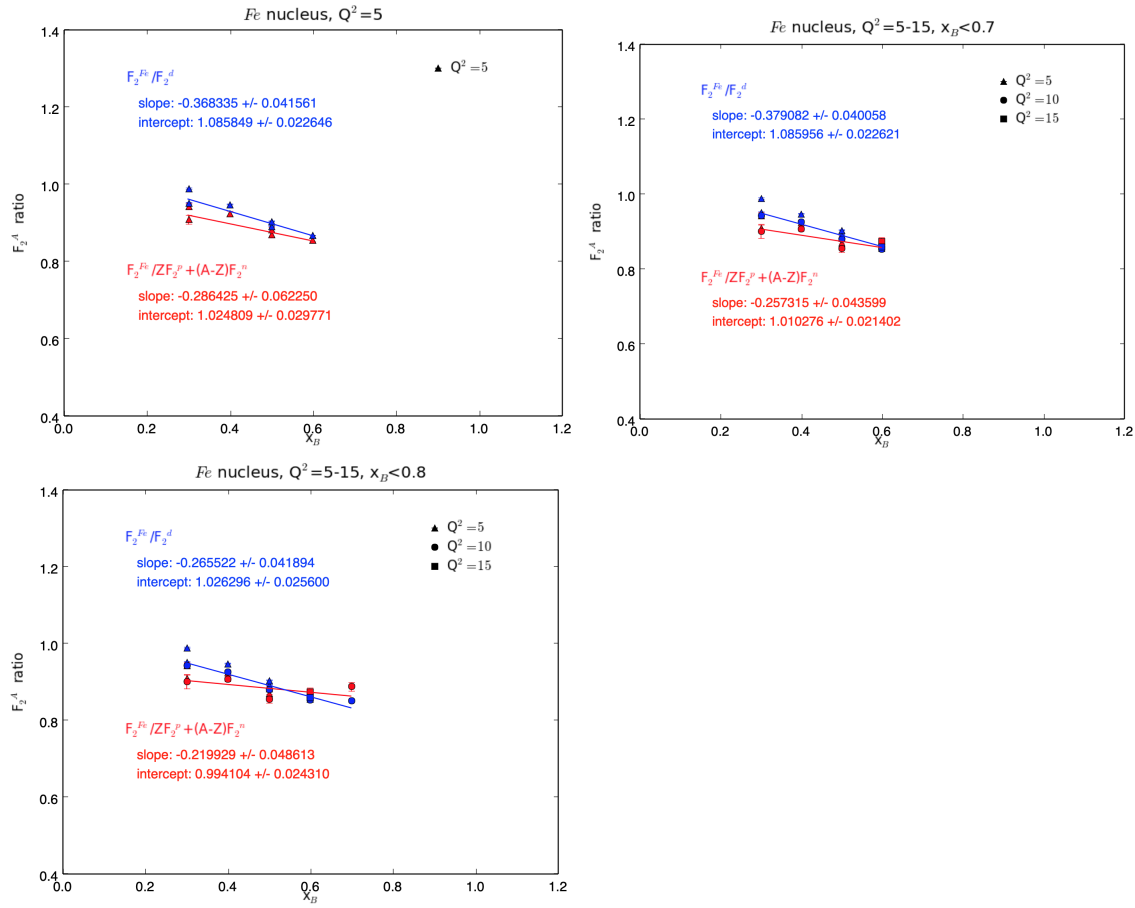


**Figure 17:** Linear fits to the Fe target data with cuts on  $Q^2$  and  $x_B$ .

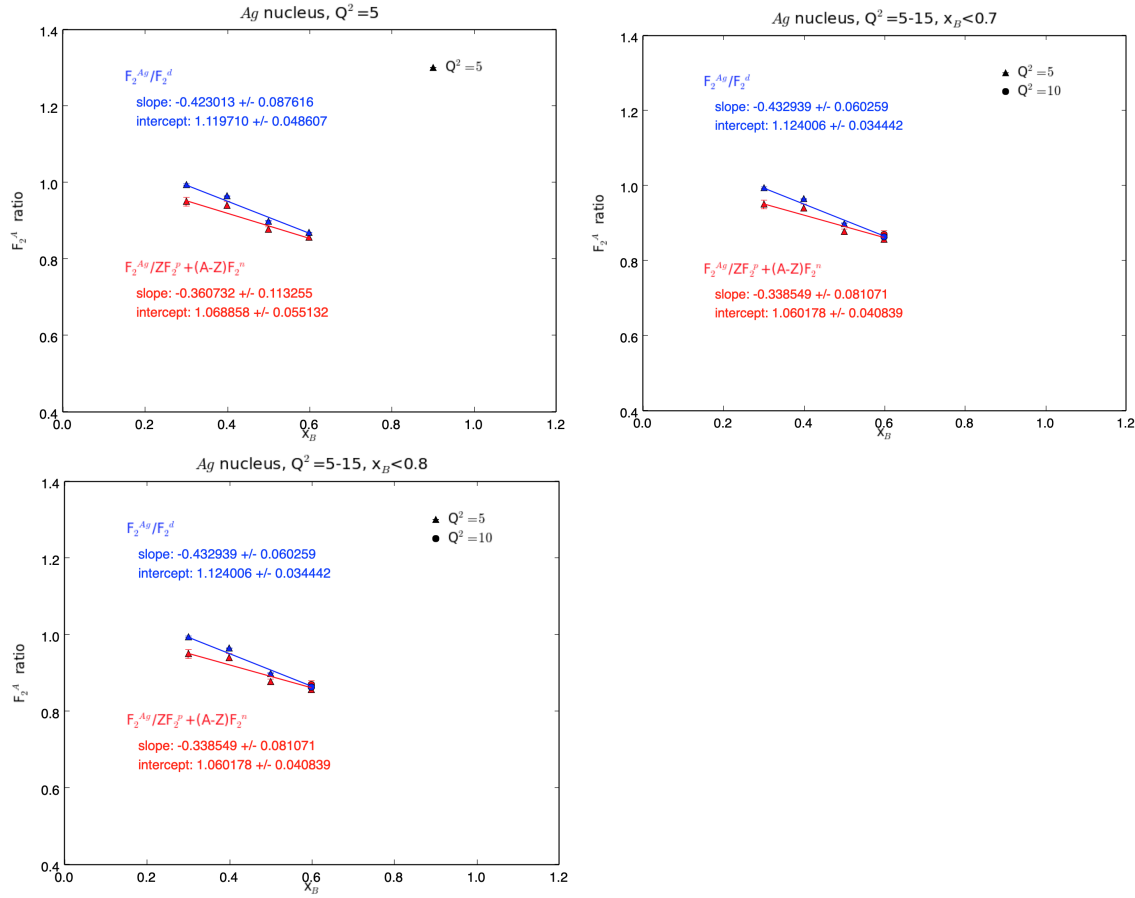


Figure 18: Linear fits to the Ag target data with cuts on  $Q^2$  and  $x_B$ .

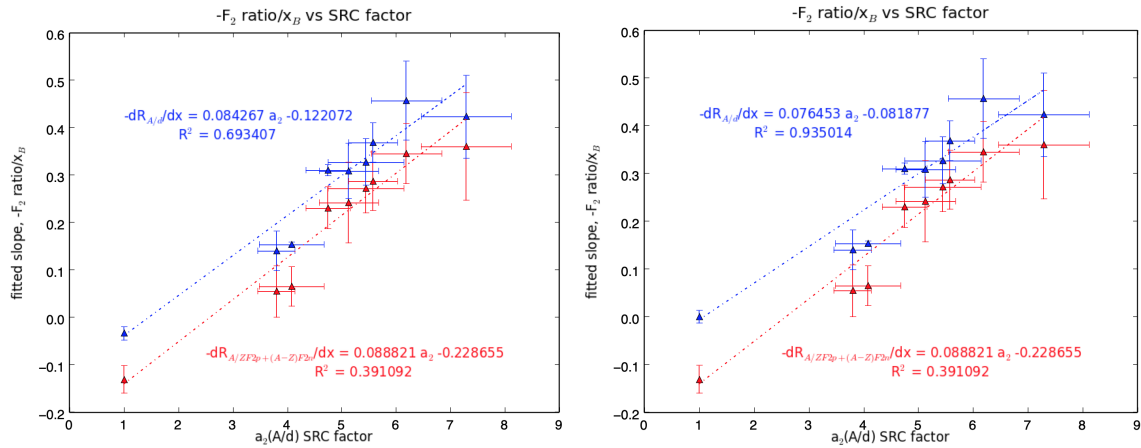


Figure 19

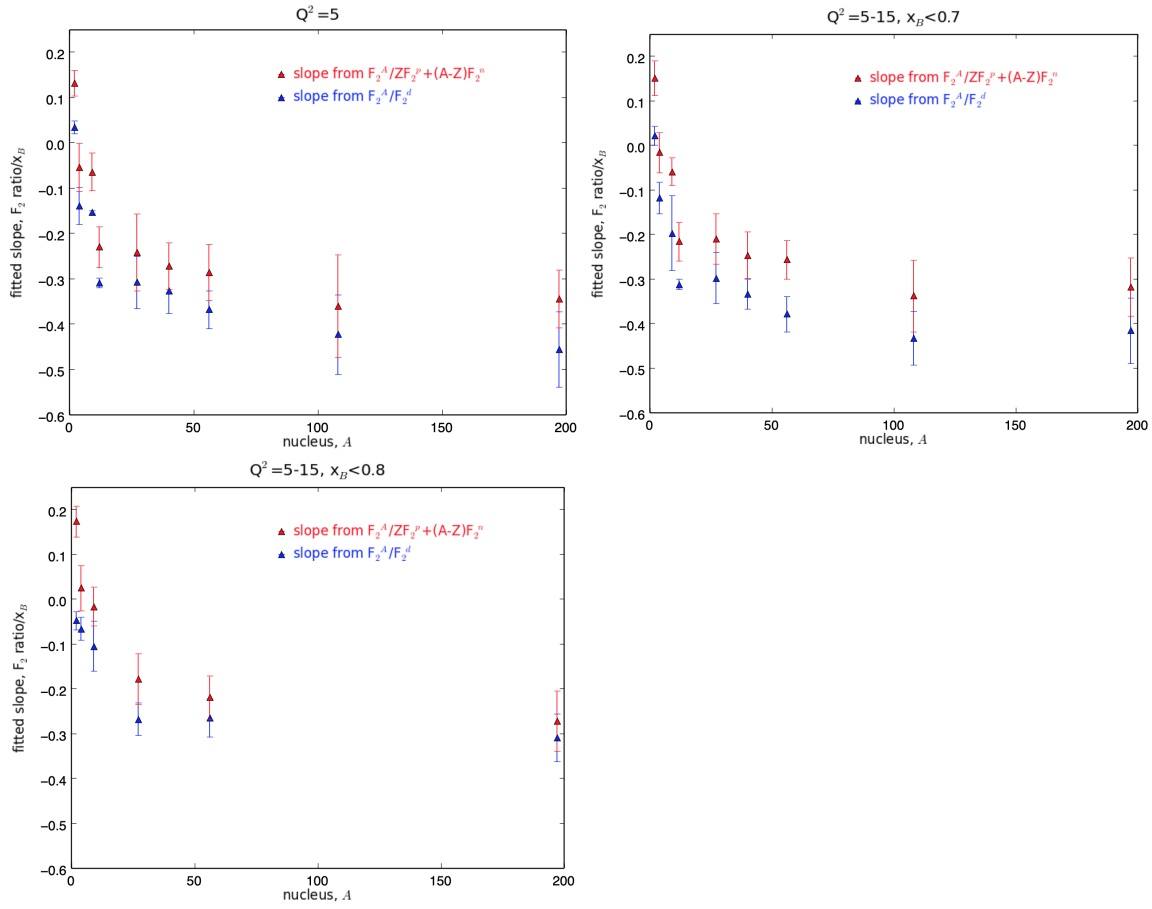


Figure 20: .

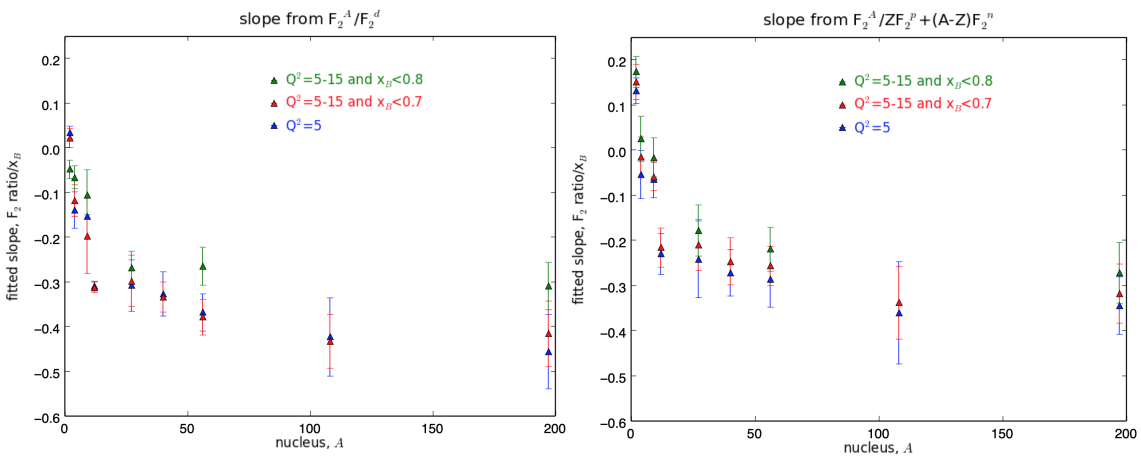


Figure 21: .